PREPARATION, CHARACTERIZATION AND APPLICATION OF SONOCHEMICALLY DOPED Fe^{3+} INTO ZnO NANOPARTICLES

Sankar Chakma[1], Jaykumar B. Bhasarkar[2], Vijayanand S. Moholkar[3]

[1,2,3] *Department of Chemical Engineering*
Indian Institute of Technology Guwahati, Guwahat –781039, Assam, India
vmoholkar@iitg.ernet.in (VSM), sankar@iitg.ernet.in (SC)

Abstract

In this present study, mechanistic investigation of ultrasound–assisted dye decolorization/degradation was investigated using sonochemically prepared Fe^{3+} doped ZnO. Fe^{3+} doped ZnO nanoparticle was prepared under ultrasound (20 kHz) irradiation using a doping concentration of 2 wt% of Fe(III). To investigate the catalytic activity of Fe^{3+} doped ZnO, Acid Red 14 (azo dye) was chosen for decolorization/degradation using sonolysis, photocatalysis and sono–photocatalysis processes. To study the influence of dopant onto structure, crystallinity, and optical properties, different analytical analyses were performed such as X–ray powder diffraction (XRD), Fourier transform infrared spectroscopy (FTIR), Zeta potential, Delsa Nano Particle Size Analyzer (PSA), Vibrating Sample Magnetometer analysis (VSM) and Field Emission Scanning Electron Microscopy (FE–SEM) etc. For photocatalytic experiments, a blended high pressure mercury UV lamp with maximum peak emission at 365 nm was used. The decolorization/degradation of dye with modified photocatalyst showed faster reaction kinetics under sono–photocatalytic process. Ultrasound showed an additive effect for degradation/decolorization process. The maximum decolorization of AR14 was achieved (~ 82%) under sono–photocatlytic process with an initial dye concentration of 20 ppm. The sono–photocatalysis process showed 1.4 – 1.6 higher reaction rates with Fe–doped ZnO than pure ZnO.

Index Terms: *ZnO, Fe–ZnO, Fe-doped ZnO, Sonocatalytic, Photocatalytic, Advanced Oxidation Process, AOP*

----------***----------

1. INTRODUCTION

In the last one decade, the synthesis or preparation of modified photcatalysts is one of the most active areas in research. The modified photocatalysts are more active in UV light as well as visible light for degradation of organic pollutants in aqueous environment. Generally, the photocatalysts have high band gap energy and so they are not much effective under visible light. Various conventional techniques or methods such as co–precipitation, sol–gel method, impregnation method, hydrothermal method etc. are used for synthesizing nanoparticles as well as synthesis of metal doped nanoparticles [1–3]. Recently, these methods are found to be more efficient for doping of metal ions for improving the photocatalytic efficiency of catalysts by decreasing the band gap which in turn increases the absorption of photons in the visible region of the light [4–7]. For doping the metal ions into semiconductor lattice, the conventional methods take much more time usually 24 – 48 h. In view of this drawback, this present study addressed a very easy and simplest technique for doping of Fe^{3+} into ZnO nanoparticles.

In order to investigate the catalytic activity of the Fe–doped ZnO, photocatalytis process (an AOP) was studied for decolorization of Acid red 14. Among the various AOPs, photocatalytic process is one of the most common advanced oxidation process (AOP) for degradation of recalcitrant pollutants. The main objective of all AOPs is the production of highly oxidizing agent such as $^{\bullet}OH$ radical for degradation of recalcitrant pollutants. Now–a–days researchers have given attention in sono–photocatalytic process, a hybrid AOP, for degradation of organic pollutants in aqueous medium. The advantage of the use of ultrasound is the facilitation of cavitation in the medium which produces various types of oxidizing species such as $^{\bullet}OH$, $HO_2^{\bullet}$, $H^{\bullet}$, $O_2^{\bullet}$ etc through transient collapse of cavitation bubble. At the moment of transient collapse of bubble, the temperature and pressure reach very high (~5000 K and ~500 bar) inside the bubble and produces highly oxidizing species. These species are generally produced by sonolysis of the water or organic solvents as indicated by our recently published paper [8]. Generally, the individual technique takes more time to mineralize the recalcitrant completely when it's applied alone, but the same could be done when two or more oxidation methods (i.e. hybrid AOP) are employed together. In the last one decade, it has been reported that by using photocatalytic process for degradation in the presence of ultrasound is more efficient than any individual AOPs [9–11]. This paper will also try to deduce the physical mechanism for decolorization of dye using sono–photocatalytic process.

2. EXPERIMENTAL SECTION

2.1 Chemicals

The following chemicals have been used for preparation of Fe–doped ZnO and decolorization of dye: ZnO (Merck), $Fe_2(SO_4)_3 \cdot H_2O$ (Merck), Acid red 14 (obtained from local market, a.b. Chemicals). For all experiments, Milli–Q water from Milli–Q Synthesis unit (Millipore®, USA) was used as the liquid medium. All the chemicals were used as received without further any pretreatment.

2.2 Preparation of photocatalyst

The one of the most popular techniques for synthesis of nano materials is impregnation method [9,12]. In order to optimize the time requirement for preparation of Fe–doped ZnO nanoparticles, Fe–doped ZnO was prepared using ultrasound–assisted impregnation method and most probably this is the first report on doping of Fe^{3+} into ZnO using ultrasound–assisted impregnation method. In this present study, the impregnation method was coupled with ultrasound to prepare nano–sized Fe–ZnO using 20 kHz frequency ultrasonic probe (Model: VCX–500, 20 kHz, 500 W). During the preparation process all the parameters were kept same as described in the literature [9]. A desired amount of previously calcined ZnO (at 400^{o}C for 5 h) was mixed with an aqueous solution of $Fe_2(SO_4)_3 \cdot H_2O$ (2 wt.%) and the solution was sonicated for 2 h using 5 sec pulse mode (5 sec on and 5 sec off mode) as mentioned by Bhatte et at. [13]. Therefore, the actual total time of sonication was 1 h. The system was operated at 40% amplitude with the theoretical dissipation rate of 200 W. Finally the supernatant was evaporated by heating the mixture at 100^{o}C overnight and was calcined at 500^{o}C for 5 h. The Fe–doped ZnO nanoparticles exhibit a color gradation from white to light yellow, which interns confirm the presence of Fe^{3+}. The experimental setup for preparation of Fe–doped ZnO nanoparticles is shown in Fig. 1.

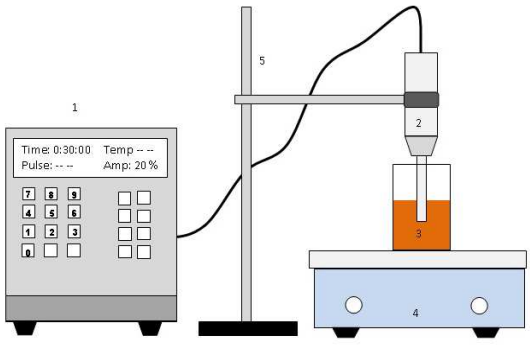

Figure 1: Experimental setup for synthesis of Fe–doped ZnO nanoparticles. (1) Ultrasonic processor, (2) ultrasonic horn, (3) reaction mixture, (4) stand for adjusting the height (5) burette stand.

2.3 Decolorization of dye

In order to study the catalytic activities of ZnO and Fe–doped ZnO, the photocatalytic experiments were carried out using 50 ml of Acid red 14 (AR14) dye solution with an initial concentration of 20 ppm. In a typical experiment, 25 mg of photocatalyst was added to AR14 dye solution and the solution was stirred for 1 hour in a dark place to reach at equilibrium adsorption–desorption condition. Then the solution was placed at the center of an ultrasound bath (Jeiotech, Capacity: 10 L) which operates at 40 kHz frequency and a power of 200 W. The temperature of the water, hence reaction solution, was maintained at 25 (±2) ^{o}C. The experiments were conducted using the following techniques: (1) sonolytic process, (2) photocatalytic process, and (3) sono–photocatalytic process. Small aliquots of sample was withdrawn in every 10 min and centrifuged using a research centrifuge (Remi, Model: R–8C) at 4500 rpm for 30 min to separate the solid catalyst particles from the sample. The filtrate was then analyzed for dye concentration using UV–Visible spectrophotometer (Model: Lambda 35). The sono–photocatalytic experiments were conducted using a blended high pressure mercury UV lamp with a peak emission wavelength of 365 nm for all experiments. All the experiments were carried out twice and the average values are taken to present the results.

3. RESULTS AND DISCUSSION

In order to investigate the changes in the crystal structure, surface morphology as well as particle size of the catalyst due to Fe^{3+} doping, different analytical measurements were employed such as X–ray power diffraction, Particle size analyzer, BET surface area, Field emission scanning electron microscopy (FE–SEM), Vibrating Sample Magnetometer etc. Then the prepared catalyst was used for degradation/ decolorization of azo dye (Acid red 14) in presence of ultrasound and UV light irradiation.

3.1. Characterization of catalyst

***Particle size analysis*:** The particle size of bare ZnO and modified Fe^{3+} doped ZnO was determined using Delsa™ Nano C (Beckman Coulter, Model: A53878) particle size analyzer. The intensity distribution of the catalysts, ZnO and Fe–doped ZnO, is shown in Fig. 2. The Fe–ZnO catalyst has a smaller and uniform particles and this effect can be attributed to the effect of sonication. During the sonication of the solution, the acoustic waves of ultrasound help to break the agglomeration of the nanoparticles. Hence, the particles remain suspended equally in the solution. The particle size distribution of prepared Fe doped catalyst (Fe–ZnO) was: D (10%) – 637.90 nm, D (50%) – 999.90 nm, and D (90%) – 1566.40 nm.

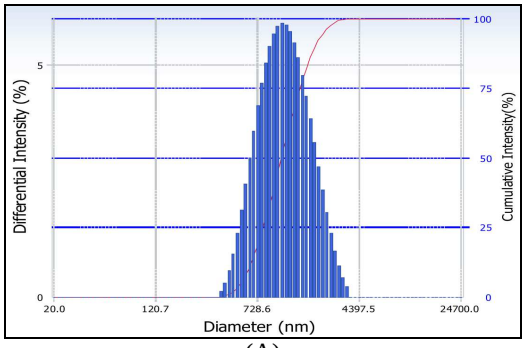

(A)

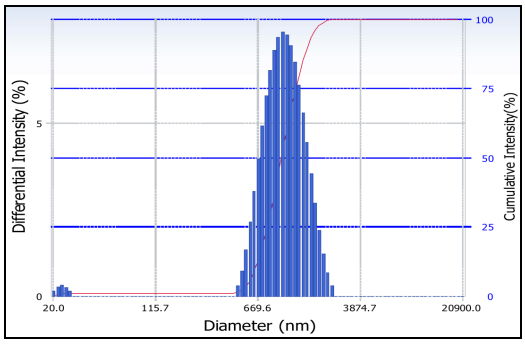

(B)

Figure 2: (A) Particle size distribution of undoped ZnO. Summary of distribution: D (10%) – 621.50 nm, D (50%) – 1110.40 nm, D (90%) – 2,026.10 nm. (B) Particle size distribution of Fe doped ZnO. Summary of distribution: D (10%) – 637.90 nm, D (50%) – 999.90 nm, and D (90%) – 1566.40 nm.

***Powder X–ray diffraction analysis*:** The structural characterization was carried out to study the changes of the crystal structure due to Fe–doped into the ZnO crystal lattice and shown in Fig. 3. As the concentration of iron was very low (2 wt %), no characteristic peaks of iron were detected in XRD pattern which was also reported by Westmoreland and Harrision [14]. The detected major peaks of the modified and unmodified products appeared to be the same. But the intensity values of the peaks were observed to be significantly increased in Fe–doped ZnO. From the XRD spectra, the characteristic peaks of undoped ZnO and Fe–ZnO were seen at 2θ values of 31.76 (100), 34.4 (002), 36.23 (101), 47.51 (102), 56.6 (110), 62.84 (103), 67.94 (112). These results correspond to a single–crystalline wurtzite structure with lattice constants: a = 3.2535 and c = 5.2151 [15]. In the modified sample, the peaks located at (002) and (101) lattice plane indicate that the hexagonal wurtzite structure is same as in undoped ZnO, where the peaks at (102) and (103) indicate wurtzite crystal structure of the sample [16]. This mean ultrasound does not effect on the crystal structure but increases crystallinity. As reported by Madhavan et al., [9]; Ahrens [17]; and Shi et al. [18], since the ionic radius of the Fe^{3+} (0.64 Å) is very close to the Zn^{2+} radius (0.60 Å), it can be assumed that Fe^{3+} can penetrate into the semiconductor lattice. The average crystallites size (D_{avg}) can also be determined from the most intense peak, corresponding to a (101) reflection using the Debye–Scherrer formula: $D_{avg} = 0.89\lambda/\beta\cos\theta$; where, λ is the X–ray wavelength of Cu–K_α, β is the line broadening at half–height and θ is the Bragg's angle of the particles.

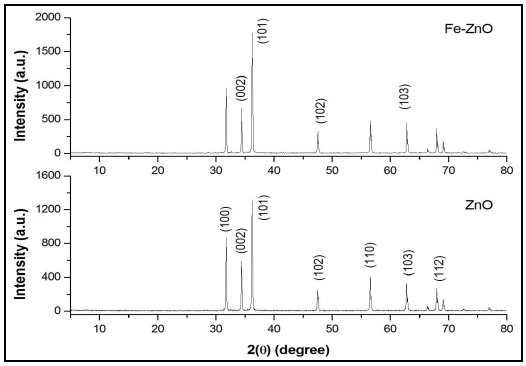

Figure 3: XRD spectrum of the undoped ZnO and Fe–doped ZnO photocatalysts.

***BET surface area analysis*:** The adsorption–desorption isotherm of N_2 were measured for undoped ZnO and Fe doped ZnO using a BET surface area analyzer (Beckman Coulter, Model: SA–3100). The BET surface area of ZnO and Fe–ZnO were 7.4 and 4.3 m^2/g, respectively. The total pore volume of the ZnO and Fe–ZnO were 0.0834 and 0.0497 cm^3/g, respectively. The reduced BET surface area of Fe–ZnO indicates that the Fe^{3+} ions are properly doped into the semiconductor lattice.

***FTIR analysis*:** To investigate the bonding configuration, infrared transmittance measurements (FTIR) were performed in the spectral range from 400–4000 cm^{-1} using Shimadzu Fourier Transform Infrared Spectrometer (Model: IRAffiniti–1). The FTIR spectra of ZnO and Fe doped ZnO is shown in Fig. 4, where a slight change in intensity was observed.

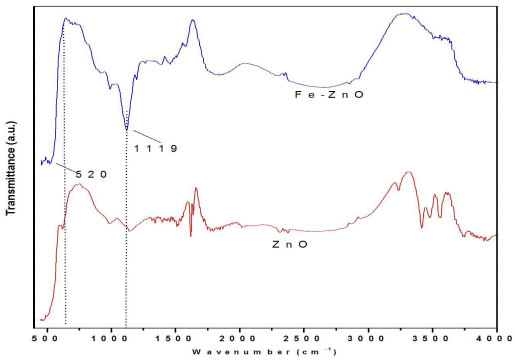

Figure 4: FTIR spectra of ZnO and Fe–ZnO photocatalysts.

In the catalyst samples (ZnO and Fe–ZnO), the peaks in the range of 400–700 cm^{-1} were attributed to ZnO stretching modes [16]. Also an additional peak was obtained in the range from 800 – 1500 cm^{-1}, which could be attributed to the incorporation of Fe^{3+} ions into the lattice position of the ZnO nano–structures [19].

***Field emission scanning electron microscopy (FE–SEM) analysis*:** The surface morphology of the ZnO and Fe–ZnO was investigated using Field Emission Scanning Electron Microscope (FESEM) and Fig. 5 shows the FESEM images of undoped ZnO and Fe–doped ZnO. From the FESEM images, it can be clearly seen that ZnO and Fe–ZnO have nearly hexagonal structure, which was also seen from XRD peak pattern of the nanoparticles (shown in Fig. 3).

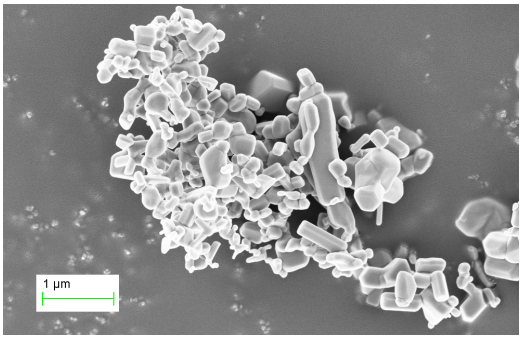

(A)

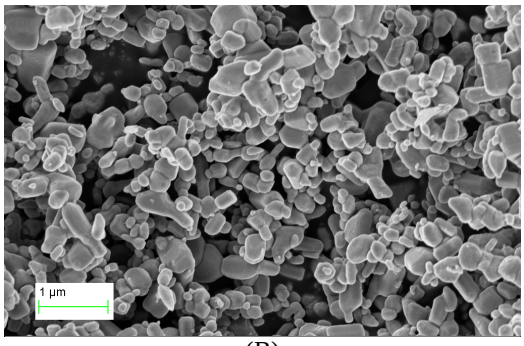

(B)

Figure 5: FESEM images of (A) ZnO and (B) Fe-doped ZnO.

***Analysis of magnetic properties*:** The magnetization versus applied magnetic field (*M–H*) curves measured at room temperature for the ZnO, Fe–ZnO(1) nanoparticles are illustrated in Fig. 6. The *M–H* curves showed that ZnO as well as Fe doped ZnO exhibit a ferro–paramagnetic behavior under the applied magnetic field in the range of –10 KOe to +10 KOe. However, more applied magnetic field is required to achieve the saturation magnetization (M_s) for ZnO and Fe–doped ZnO [1–3]. The coercivities of pure ZnO and Fe doped ZnO are found to be ~ 55 Oe and ~ 100 Oe, respectively.

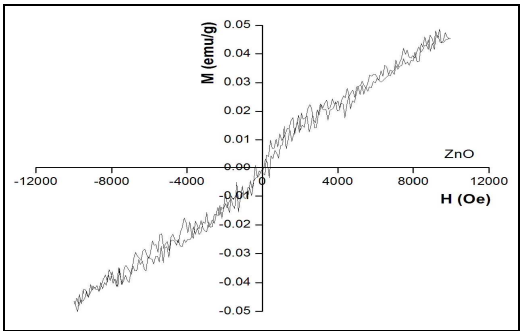

(A)

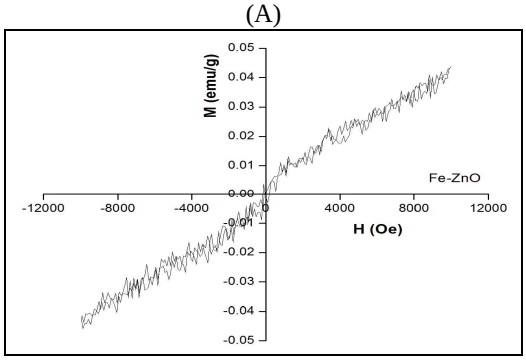

(B)

Figure 6: M–H curves of undoped ZnO and Fe–doped ZnO nanoparticles

***Surface charge analysis*:** The change in charge due to doping of Fe^{3+} on the surface of the nanoparticles was analyzed using Beckman Coulter Zeta Potential analyzer. All the measurement was carried out with water at neutral pH value. The zeta potential of pure ZnO was 20 mV, while the zeta potential for Fe–ZnO was 20.45 mV. This value of zeta potential of ZnO at neutral pH was also reported by Chang and Tsai [20]. The analysis showed the charge on the surface of the nanoparticles does not change due to iron doping.

3.2. Decolorization of Acid red 14 dye

To investigate the catalytic activity of the prepared Fe doped ZnO photocatalyst, we have considered Acid red 14 (an azo dye) for decolorization/degradation using photocatalysis process. The experiments were carried in three categories, viz. sonolytic, photocatalytic, and sono–photocatalytic. Table 1 shows a comparison of decolorization/degradation results under various experimental categories obtained with ZnO and Fe–ZnO. The catalytic activity of Fe–doped ZnO was found to be always faster than that of undoped ZnO. The sonolytic process alone gives a decolorization efficiency of 14.2%, while maximum decolorization of AR14 was achieved under sono–photocatlytic process (82% with ZnO and ~81% with Fe–ZnO). Although, the both catalyst ZnO and Fe–ZnO showed almost same total highest decolorization efficiency, but when the reaction is considered for initial first 10 min it can be observed that the decolorization efficiency of Fe–ZnO is always greater than that of ZnO. The following features

were found for degradation of dye: (1) the sonolysis process is able to degrade the dye upto 14.2% in 1 h of sonication. For higher extend of degradation of recalcitrant pollutants, sonolysis process needs more time, (2) in conventional photocatalysis process, the total decolorization efficiency for both the catalysts were almost same. However, Fe–ZnO showed a moderately higher and faster decolorization rate than the decolorization with ZnO, (3) in sono–photocatalysis process, ~18% increase in total decolorization/ degradation efficiency was seen within initial 10 minute of the reaction under UV light irradiation with Fe–doped ZnO than that obtained with ZnO in 10 minute.

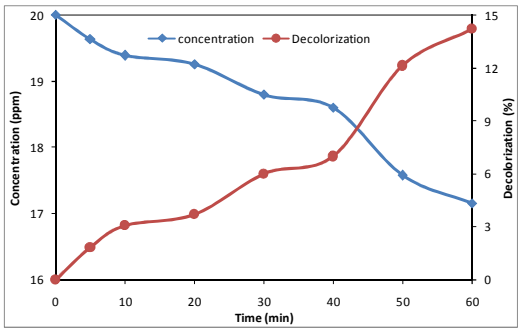

Figure 7: Time history of Acid red 14 decolorization using sonolysis process. Conditions: $[AR14]_0$: 20 ppm, f = 40 kHz

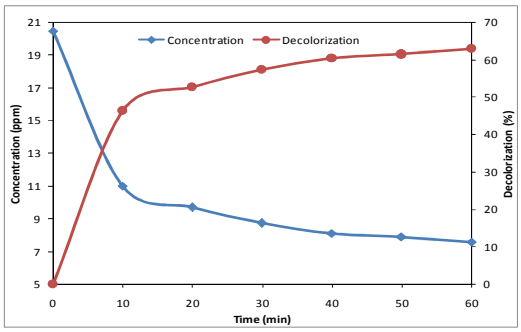

(A)

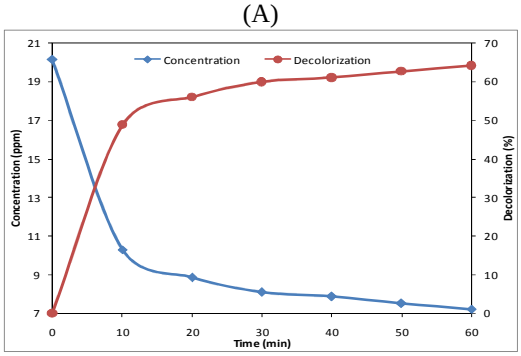

(B)

Figure 8: Time history of decolorization of AR14 under conventional photocatalysis process. The reaction composition of the mixture: $[AR14]_0$: 20 ppm, [ZnO] & [Fe–ZnO]: 25 mg.

The higher decolorization efficiency of dye under sono–photocatalytic process could the attributed to $^{\bullet}OH$ radical produced during transient collapse of cavitation bubble through the following reaction:

$$H_2O \xrightarrow{US} H^{\bullet} + {}^{\bullet}OH$$

$$2\ {}^{\bullet}OH \longrightarrow H_2O_2$$

This $^{\bullet}OH$ radicals directly attack to the dye molecules, which results increase in decolorization process. Also extra $^{\bullet}OH$ radicals are formed due to photolysis of H_2O_2 generated through sonolysis of water during the sono–photocatalysis process. Chemical effects of cavitation, at which temperature and pressure reach ~5000 K and ~500 bar inside the bubble [21–23], is the principal phenomenon behind of all these reason. The overall dye degradation/ decolorization rate by sono–photocatalytic process is faster and higher than in any other individual process for dye decolorization.

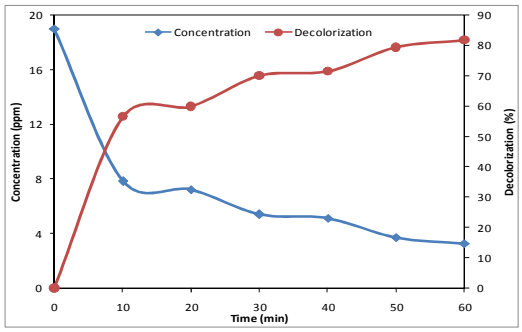

(A)

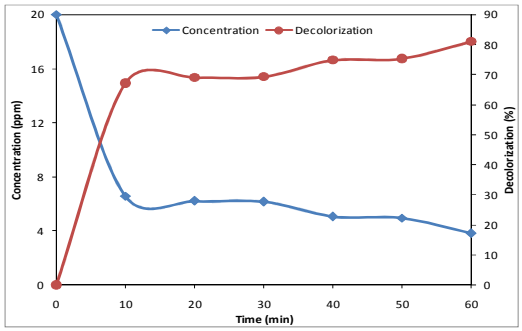

(B)

Figure 9: Time history of decolorization of AR14 under sono–photocatalytic process with (A) ZnO, (B) Fe–ZnO. Reaction soln.: $[AR14]_0$: 20 ppm, [ZnO] & [Fe–ZnO]: 25 mg.

Table 1: Summary of experimental results for decolorization of Acid red 14

Experimental category	Decolorization (η) $		k (s^{-1}) #			
1. Sonication alone	14.21		4×10^{-5} ($R^2 = 0.95$)			
	Decolorization (η) and Kinetic constant (k)					
	ZnO			Fe–ZnO		
	10 min	60 min	k (s^{-1}) #	10 min	60 min	k (s^{-1}) #
2. Conventional photocatalytic process	46.0	62.93	6.28×10^{-4} ($R^2 = 0.84$)	49.0	64.04	6.87×10^{-4} ($R^2 = 0.85$)
3. Sono–photocatalytic process	56.46	81.68	8.72×10^{-4} ($R^2 = 0.88$)	67.08	80.92	1.11×10^{-3} ($R^2 = 0.81$)

– k is the pseudo 1st order kinetic constant in (s^{-1}), R^2 is the regression coefficient, $ – η is the decolorization efficiency in (%)

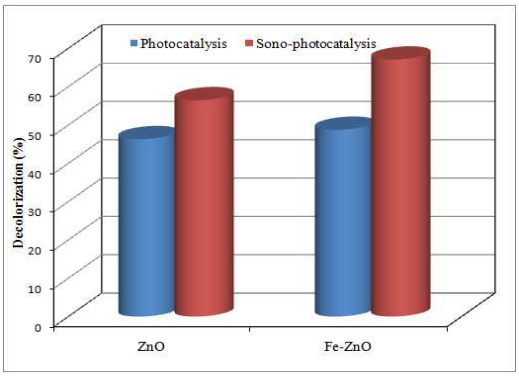

Figure 10: Comparision between conventional photocatalysis and sono-photocatalysis processes using ZnO and Fe-ZnO.

Fig. 10 shows the comparision between conventional photocatalysis and sono-photocatalysis processes with different catalysts, viz. ZnO and Fe-doped ZnO. A significant increase in decolorization was seen with modified Fe-doped ZnO as compared to bare ZnO. Also, the maximum decolorization was obtained with Fe-ZnO under sono-photocatalysis process.

3.3. Determination of reaction kinetic

The chemical reaction kinetic constant of overall reaction was determined by assuming that the reaction is pseudo 1st order reaction. The following equation was used to calculate the kinetic constant for decolorization of Acid red 14:

$$-\ln(1-X) = kt$$

where, X is the degradation/ decolorization of AR14 at any time t in sec. By plotting $-\ln(1-X)$ vs. t, one can easily estimate the kinetic constant k as slope from the graph. The summery of reaction kinetic constant with regression coefficient is shown in Table 1. The reaction kinetic obtained with Fe–doped ZnO is always higher than that of undoped ZnO. The reaction kinetic with Fe–ZnO is 1.1 – 1.3 times greater than that of reaction kinetics obtained with ZnO, the sono–photocatalysis process gave 1.4 – 1.6 higher reaction rates with Fe–ZnO than ZnO.

CONCLUSIONS

This present study showed a very easy and simplest technique for doping of Fe^{3+} into the semiconductor lattice within a short period of time. The sonolysis process alone is able to decolorize the dye, but the process needs more for higher extend of decolorization. The hybrid sono–photocatalytic process showed ~1.3 time higher degradation/decolorization efficiency than the conventional photocatalytic process. The modified Fe–doped ZnO catalyst showed an additives effects for degradation of Acid red 14 in presence of ultrasound irradiation. Moreover, ultrasound helps to accelerate the catalytic process by producing extra oxidizing ($^{\bullet}OH$) through transient collapse of cavitation bubbles. Under UV light irradiation, the reaction kinetic was 1.28 times higher with Fe–ZnO than that of ZnO under the same reaction conditions. The present technique, i.e. ultrasound–assisted impregnation technique, can be useful for doping of other metal ions which generally require more time to penetrate and settle properly into the semiconductors such as ZnO and TiO_2 etc.

ACKNOWLEDGEMENT

Authors of the paper sincerely acknowledge to Central Instruments Facility, I.I.T Guwahati for providing analytical facilities to characterize the samples.

REFERENCES

[1] H–W Zhang, Z–R Wei, Z–Q Li, G–Y Dong, Room–temperature ferromagnetism in Fe–doped, Fe– and Cu–codoped ZnO diluted magnetic semiconductor, Mater. Lett. 61 (2007) 3605–3607.

[2] D. Wang, Z.Q. Chen, D.D. Wang, J. Gong, C.Y. Cao, Z. Tang, L.R. Huang, Effect of thermal annealing on the structure and magnetism of Fe–doped ZnO nanocrystals synthesized by solid state reaction, J. Magn. Magn. Mater. 322 (2010) 3642–3647.

[3] D.A.A. Santos, M.A. Macedo, Study of the magnetic and structural properties of Mn–, Fe–, and Co–doped ZnO powder, Physica B 407 (2012) 3229–3232.
[4] M. Samadi, H. Asghari Shivaee, M. Zanetti, A. Pourjavadi, A. Moshfegh, Visible light photocatalytic activity of novel MWCNT–doped ZnO electrospun nanofibers, J. Molecul. Catal. A 359 (2012) 42–48.
[5] A. Mills and L.H. Stephen, An overview of semiconductor photocatalysis, J. Photochem. Photobiol. A: Chem. 108 (1997) 1–35.
[6] O. Carp, C.L. Huisman, A. Reller, Photoinduced reactivity of titanium dioxide, Prog. Solid State Chem. 32 (2004) 33–177.
[7] H. Fang, K.V.S. Rao, S. Madapusi, R. Dharmarajan, N. Ravi, Tailored titanium dioxide photocatalysts for the degradation of organic dyes in wastewater treatment: a review, Appl. Catal. A: General 359 (2009) 25–40.
[8] S. Chakma, V.S. Moholkar, Numerical simulation and investigation of system parameters of sonochemical process, Chin. J. Eng. (2013) ID: 362682.
[9] J. Madhavan, P.S. Sathish Kumar, S. Anandan, M. Zhou, F. Grieser, M. Ashokkumar, Ultrasound assisted photocatalytic degradation of diclofenac in an aqueous environment, Chemosphere 80 (2010) 747–752.
[10] E. Selli, C.L. Bianchi, C. Pirola, G. Cappelletti, V. Ragaini, Efficiency of 1,4–dichlorobenzene degradation in water under photolysis, photocatalysis on TiO_2 and sonolysis, J. Hazard. Mater. 153 (2008) 1136–1141.
[11] Y.C. Chen, A.V. Vorontsov, P.G. Smirniotis, Enhanced photocatalytic degradation of dimethyl methylphosphonate in the presence of low frequency ultrasound, Photochem. Photobiol. Sci. 2 (2003) 694–698.
[12] R.I. Bickley, J.S. Lees, R.J.D. Tilley, L. Palmisano, and M. Schiavello, Characterisation of iron/titanium oxide photocatalysts part 1 .–structural and magnetic studies, J. Chem. Soc. Faraday Trans., 88 (1992) 377–383.
[13] K.D. Bhatte, S–I Fujita, M. Arai, A.B. Pandit, B.M. Bhanage, Ultrasound assisted additive free synthesis of nanocrystalline zinc oxide, Ultrason. Sonochem. 18 (2011) 54–58.
[14] P.R. Westmoreland, D.P. Harrision, Evaluation of candidate solids for high temperature desulfurization of low–Btu gases, Environ. Sci. Technol. 10 (1976) 659–661.
[15] H. Kim, B.K. Lee, K–S An, S. Ju, Direct growth of oxide nanowires on CuO_x thin film, Nanotechnology 23 (2012), ID: 045604.
[16] R. Saleh, N.F. Djaja, S.P. Prakoso, The correlation between magnetic and structural properties of nanocrystalline transition metal–doped ZnO particles prepared by the co–precipitation method, J. Alloy. Compound. 546 (2013) 48–56.
[17] L.H. Ahrens, The use of ionization potentials: part 1. Ionic radii of the elements, Geochim. Cosmochim. Acta 2 (1952) 155–169.
[18] Z. Shi, D. Liu, X. Yan, Z. Gao, S. Bai, Growth and properties analysis of metalorganic chemical vapor deposited $Mg_xZn_{1-x}O$ films on C–Al_2O_3 substrates, Front. Mech. Eng. China 3 (2008) 261–264.
[19] T. Pandiyarajan, R. Udayabhaskar, B. Karthikeyan, Role of Fe doping on structural and vibrational properties of ZnO nanostructures, Appl. Phys. A 107 (2012) 411–419.
[20] H. Chang, M–H Tsai, Synthesis and characterization of ZnO nanoparticles having prism shape by a novel gas condensation process, Rev. Adv. Mater. Sci. 18 (2008) 734–743.
[21] S. Chakma, V.S. Moholkar, Physical mechanism of sono–fenton process, AIChE J. (2013), doi:10.1002/aic.14150.
[22] J.B. Bhasarkar, S. Chakma, V.S. Moholkar, Mechanistic features of oxidative desulfurization using sono–fenton–peracetic acid (ultrasound/Fe^{2+}–CH_3COOH–H_2O_2) system, Ind. Eng. Chem. Res. (2013) DOI: 10.1021/ie400879j.
[23] H.A. Choudhury, S. Chakma, V.S. Moholkar, Mechanistic insight into sonochemical biodiesel synthesis using heterogeneous base catalyst, Ultrasonic. Sonochem. (2013), http://dx.doi.org/10.1016/j.ultsonch.2013.04.010.

BIOGRAPHIES

Mr. S. Chakma is a research scholar in Department of Chemical Engineering at I.I.T. Guwahati, India. He is a recipient of "Ambuja Young Researcher's Award" given by Indian Institute of Chemical Engineers (IIChE).

Mr. J.B. Bhasarkar is a research scholar of Chemical Engineering Department, I.I.T. Guwahati. He obtained his M.Tech from I.I.T. Roorkee.

Dr. V.S. Moholkar is a Professor and Head of the Department of Chemical Engineering at Indian Institute of Technology Guwahati, India. He has to his credit 74 publications in peer reviewed international journals with more than 1000 citations.